Energy Harvesting Aided by Random Motion; A Stochastic Geometry Based Approach

S. Kusaladharma and C. Tellambura, *Fellow*, *IEEE*
Department of Electrical and Computer Engineering
University of Alberta, Edmonton, Alberta T6G 2V4, Canada
Email: kusaladh@ualberta.ca and chintha@ece.ualberta.ca

***Abstract*—RF energy harvesting is a promising solution to increase the battery life and energy efficiency of device-to-device (D2D) and sensor devices. To this end, this paper analyzes the energy harvesting performance of a mobile D2D device exclusively powered by energy harvesting from underlying cellular base stations. A homogeneous Poisson point process is used to model base stations while a modified random waypoint model is used for the D2D motion. We derive the probability of a D2D device being within a harvesting region surrounding base stations after multiple transitions, and the steady state probability of being fully charged using a Markov chain based approach. It is shown that the number of transitions required to be within a harvesting region is increases significantly when the harvesting threshold power level goes beyond -55 dB.**

***Index Terms*—Energy harvesting, Random motion, Stochastic geometry**

I. Introduction

Radio frequency (RF) energy harvesting for low powered wireless devices is an attractive concept to improve their performance and to reduce the carbon footprint [1], [2]. RF energy harvesting is suitable over other renewable sources such as solar or wind energy because it is less affected by atmospheric and geographical conditions [3]. While RF energy harvesting can be based on either dedicated transmitters or ambient RF sources, the second option is preferable for applications such as sensor networks due to cost savings and the self sustaining nature [3], [4]. Significant work has been accomplished in the development of receiver technology; prototypes have been tested which can can harvest up to $100\mu W$ at ambient energy densities of $40\mu W cm^{-2}$ [3].

The significant challenge of RF energy harvesting from ambient sources such as cellular networks is its inherent uncertainty [5]. For example, the distances from the ambient base stations play a key role in the power intensity at a receiver. However, modern wireless networks are increasingly stochastic in nature [6], and channel uncertainties complicate things. But, if the energy harvesting devices are mobile[1], this ability can be used to improve the harvesting performance. To this end, this letter investigates the feasibility of energy harvesting for motion enabled devices.

Energy harvesting performance of sensor and device-to-device (D2D) nodes have been popular topics of past research. For example, [4] proposes a novel network model which uses stochastic geometry to analyze energy harvesting devices co-existing with a primary network, while [5] extends this model by incorporating path loss inversion based power control and incomplete power depletions. Meanwhile references [6], [7] develop energy harvesting protocols when D2D devices harvest energy from a multi channel cellular network. Moreover, [8] characterizes network performance when relay devices harvest energy, and analytically model the harvested energy incorporating temporal correlations using Markov chains. An energy field model is introduced in [9] to analyze the coverage probability of a network powered by ambient energy harvesting. The authors of [10] incorporate user mobility in characterizing the energy harvesting performance, and show that mobility can indeed be beneficial.

Even though there is a wealth of research on energy harvesting, to the best of our knowledge only [10] has attempted to improve the energy harvesting performance via the device's mobility. However, the authors only assume a single transmitting base station which acts as a dedicated power source. So, how would motion affect the harvesting performance from multiple ambient RF sources which are randomly located? Furthermore, how do temporal correlations affect the harvesting performance? These are critical questions that we seek answers within this letter.

To this end, we consider a random set of cellular base stations in $\mathcal{R}^2$ modelled stochastically as a Poisson point process (PPP). These base stations transmit their signals which are subject to fading and log-distance path loss. The energy harvesting devices can harvest energy as long as they are within specific harvesting zones around the base stations where the received ambient RF power is greater than the threshold power level required for their conversion circuits to operate. Whenever a device is outside the harvesting region, it conducts a random motion till it's within the harvesting region. Using tools from stochastic geometry, we derive the probability of a device being within a harvesting region. Furthermore, using a Markov chain based approach, we derive the steady state transmission probability after considering temporal effects.

II. System Model

A. Spatial Model

We consider a system where energy harvesting nodes are co-located with an overlaying cellular network spanning $\mathbb{R}^2$ (Fig. 1). The cellular network is composed of base stations and user devices which are located randomly. While the locations of base stations are traditionally pre-planned, the advent of small cells, femto access points, and heterogeneous networks have made modern wireless networks inherently random. On the other hand, the locations of cellular users and energy harvesting devices are always random. As such, mathematical approaches such as stochastic geometry must be used to

[1]Devices can either be user held or mounted on autonomous robots or vehicles.

This article has been accepted for publication in a future issue of this journal, but has not been fully edited. Content may change prior to final publication. Citation information: DOI 10.1109/TGCN.2020.2994513, IEEE Transactions on Green Communications and Networking

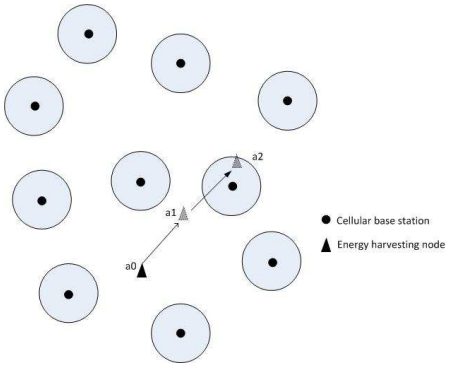

Fig. 1: System model. The shaded regions surrounding the cellular base stations represent the harvesting zones. The energy harvesting node initially located at $a0$ conducts a motion; first to $a1$ and subsequently to $a2$. As $a2$ is within the harvesting zone, it concludes its motion there. Only a single energy harvesting node is represented for clarity.

model such networks. Therefore, we will model the cellular base stations using homogeneous PPPs [11]. The PPP can accurately model even pre-planned wireless networks while allowing tractable analysis, which has made it popular among researchers. In a homogeneous PPP with node density per unit area λ, the probability of having k nodes within a given area $\mathcal{A}$ ($\Pr[N(\mathcal{A}) = k]$) is given by [11]

$$\Pr[N(\mathcal{A}) = k] = \frac{(\lambda\mathcal{A})^k}{k!} e^{-\lambda\mathcal{A}}. \tag{1}$$

As such, let the PPP of cellular base stations be Φ_{cb} with a density of λ_{cb}. It should noted that because homogeneous PPPs are used, λ_{cb} is constant over all $\mathbb{R}^2$. Similarly, let the cellular receivers form a PPP of Φ_{cu} with density λ_{cu}. The energy harvesting nodes also form their own PPP Φ_{eh} with density λ_{eh}.

In the cellular system, the users connect with their closest base station. Thus, the base stations form Voronoi cells. We assume without the loss of generality that all cellular base stations transmit whenever there is a cellular receiver within its cell. In other words, the cellular users are always active. If activity factors were considered, they can be easily incorporated by thinning the PPP of cellular users as necessary. For example, for a user activity factor of κ, the active cellular users form a homogeneous PPP with density $\kappa\lambda_{cu}$.

B. Signal Model

In this work, we will consider the downlink channel, and we assume full frequency reuse. Furthermore, each base station is assumed to serve only a single user. However, multiple user devices being served by a base station can be easily incorporated [6]. Each cellular base station transmits at power P. While power control procedures are the norm in modern networks [12], we leave it open as a future work.

The signals are subject to Rayleigh fading and log-distance path loss. With Rayleigh fading, the channel power gain is denoted by $|h|^2$, $f_{|h|^2}(x) = e^{-x}, 0 \leq x \leq \infty$. The fading is assumed to be independent between different pairs of users. With log distance path loss, the received power P_R at a distance r from the transmitter is given by $P_R = Pr^{-\alpha}$, where P is the transmit power and α is the path loss exponent.

C. Energy Harvesting and Network Operation

The downlink transmission phase of the cellular network is divided into time slots of duration T. It should be noted that these time slots can refer to frames or super frames without the loss of generality for the purposes of this letter. We further assume that all cellular base stations are fully synchronized, and that the energy harvesting nodes also get synchronized with the cellular network for the purposes of energy harvesting.

The energy harvesting nodes are solely powered through ambient RF energy from the cellular base stations. However, due to practical requirements of the energy harvesting circuitry, the ambient received power has to be greater than a certain threshold to harvest energy. Let this level be P_γ. If $\mathcal{D}_t$ is any energy harvesting node located at x, and the location of a cellular base station is y_j where $y_j \in \Phi_{cb}$, the distance between $\mathcal{D}_t$ and the j-th cellular base station r_j is written as $r_j = ||x - y_j||$. Energy harvesting is possible from the j-th cellular base station whenever the average received power is greater than the energy harvesting threshold. This criterion can be formally expressed as $Pr_j^{-\alpha} > P_\gamma$. It should be noted that small scale fading has been omitted from the criterion because it averages to 1 within a specific time slot. Thus, for the purposes of this letter, the channel coherence time is significantly lower than T. For $\mathcal{D}_t$ to harvest sufficient energy from the j-th cellular base station, it should be within a distance of $r_j = \left(\frac{P}{P_\gamma}\right)^{\frac{1}{\alpha}}$ from it. Generalizing this concept, for $\mathcal{D}_t$ to harvest energy from any cellular base station, it has to be within a harvesting region $\mathcal{H}$ where $\mathcal{H} = \bigcup_{j\in\Phi_{cb}} b(y_j, r_j)$. Here $b(y_j, r_j) \in \mathbb{R}^2$ denotes a disc shaped area of radius r_j surrounding y_j. Furthermore, whenever $\mathcal{D}_t$ is within the harvesting region $\mathcal{H}$, the harvested energy per time slot is assumed to remain the same irrespective of the distance to the cellular base station or whether there are two or more base stations within $\left(\frac{P}{P_\gamma}\right)^{\frac{1}{\alpha}}$ from $\mathcal{D}_t$.

In this letter, we assume that $\mathcal{D}_t$ needs to be within a harvesting region for N time slots in order to fully charge its batteries. Unless fully charged, no transmission occurs from $\mathcal{D}_t$. When fully charged, $\mathcal{D}_t$ conducts its transmission during the next time slot whenever there is data to be transmitted. We assume that a full depletion of power takes place after a transmission, and that $\mathcal{D}_t$ will begin the energy harvesting phase again. As our focus is on investigating the energy harvesting success, we do not look into the dynamics of the transmitted signal by $\mathcal{D}_t$ for brevity. Therefore, receiver or sink node selection criteria or power control schemes by $\mathcal{D}_t$ are not considered. However, incorporating these factors would be interesting research challenges for the future.

The energy harvesting nodes are assumed to be mobile, while the cellular base stations are stationary. However, in the energy harvesting stages, $\mathcal{D}_t$ will be static as long as its within a harvesting region. We will assume a modified version of the random waypoint model [13], [14] to model movements. The specific protocol is described below.

This article has been accepted for publication in a future issue of this journal, but has not been fully edited. Content may change prior to final publication. Citation information: DOI 10.1109/TGCN.2020.2994513, IEEE Transactions on Green Communications and Networking

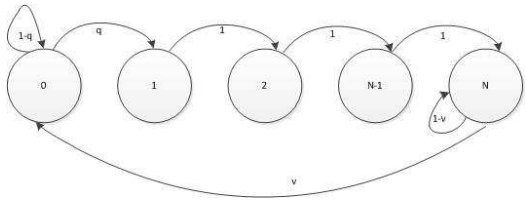

Fig. 2: Markov chain model with 0 being the uncharged state and N being the fully charged state.

- When $\mathcal{D}_t$ has depleted it's power after a previous transmission, it checks whether it's location x is within the harvesting region $\mathcal{H}$.
- If $x \in \mathcal{H}$, energy is harvested for N time slots. $\mathcal{D}_t$ remains static till the harvesting procedure is complete.
- If $x \notin \mathcal{H}$, $\mathcal{D}_t$ travels for 1 time slot at any random direction θ with velocity v. If x_1 is the location of $\mathcal{D}_t$ afterwards, it checks whether $x_1 \in \mathcal{H}$. If yes, energy is harvested for N time slots. If not, $\mathcal{D}_t$ travels in the same angle θ at velocity v for another time slot. This process continues till $\mathcal{D}_t$ is within the harvesting region (Fig. 1).
- After the harvesting is complete, $\mathcal{D}_t$ can either remain stationary or move about either randomly or depending on its requirements till its transmission is complete.

III. Steady State Transmission Probability

In this section we will derive the steady state transmission probability of $\mathcal{D}_t$. Let this probability be denoted as p_{st}. p_{st} depends on the probability that $\mathcal{D}_t$ is fully charged (p_c), and the probability that $\mathcal{D}_t$ has data to transmit (ν). It should be noted that ν depends on the specific traffic generation and receiver association models which are out of the scope of this paper. On the other hand, p_c depends on temporal effects, and a Markov chain based analysis is needed.

Fig. 2 represents the state transition diagram for the energy harvesting process. The Markov chain has $N+1$ levels as we assume $\mathcal{D}_t$ needs N charging slots. The state 0 represents the uncharged state while state N represents the fully charged state. The probability of transitioning from state 0 to state 1 is represented as q. q depends on the probability of being within the harvesting region, and will be analyzed in the subsequent section. As $\mathcal{D}_t$ remains static once within a harvesting region, the probability of transitioning from state k to $k+1$ where $1 \leq k \leq N-1$ after a subsequent time slot is 1. When $\mathcal{D}_t$ is fully charged (i. e. in state N) the transition probability is ν. The overall procedure can be represented in matrix form as follows where Q is the state transition matrix.

$$Q = \begin{bmatrix} 1-q & q & 0 & 0 & . & 0 \\ 0 & 0 & 1 & 0 & . & 0 \\ 0 & 0 & 0 & 1 & . & 0 \\ . & . & . & . & . & . \\ \nu & 0 & 0 & . & . & 1-\nu \end{bmatrix}.$$

The probability p_c is the steady state probability of $\mathcal{D}_t$ being within state N. If $\omega = [\omega_0\ \omega_1\ ..\ \omega_N]$ is the vector of steady state probabilities, we may write $\omega = Q\omega$ at steady state. Thus, we can obtain

$$p_c = \omega_N = \frac{q}{q + \nu + (N-1)q\nu}. \tag{2}$$

IV. Probability of Being Within the Harvesting Region

In this section, we derive the probability of $\mathcal{D}_t$ being within the harvesting region $\mathcal{H}$ (q). Without the loss of generality, let $\mathcal{D}_t$ be located initially at the origin. As mentioned in Section II, $\mathcal{D}_t$ conducts a motion in each time slot till it comes within a harvesting region. Therefore, the probability of $\mathcal{D}_t$ being within $\mathcal{H}$ after each subsequent time slot needs to be taken into account for the derivation of q. Thus, we can approximately write

$$q = \frac{1}{W+1}, \tag{3}$$

where W is the average number of required transitions. W can be written as

$$W = \sum_{t=0}^{\infty} t q_t \prod_{s=0}^{t-1} (1 - q_s), \tag{4}$$

where $q_*(* \in \{t, s\})$ is the probability that $\mathcal{D}_t$ is within $\mathcal{H}$ before the $t+1$-th time slot, and t is the number of time slots that $\mathcal{D}_t$ conducts a motion.

The special probability q_0 is the probability of $\mathcal{D}_t$ being within $\mathcal{H}$ at the onset. Using the void probability of PPPs, we can obtain q_0 as the complement of having 0 cellular base stations within $b(0, r_j)$. Thus, we have

$$q_0 = 1 - e^{-\pi \lambda_{cb} \left(\frac{P}{P_\gamma}\right)^{\frac{2}{\alpha}}}. \tag{5}$$

Now, in order to find q_s for $s > 0$, we need the distribution of the distances from $\mathcal{D}_t$ to the cellular base stations. If r_k is the distance from the origin (the initial location of $\mathcal{D}_t$) to the k-th nearest cellular base station (denoted as $\mathcal{C}_k$), r_k is distributed as [12], [15]

$$f_{r_k}(x) = \frac{2(\pi \lambda_{cb})^k}{(k-1)!} x^{2k-1} e^{-\pi \lambda_{cb} x^2}, 0 < x < \infty. \tag{6}$$

Because the cellular base stations are stationary, the distance distributions will change whenever $\mathcal{D}_t$ moves at velocity v at an angle θ. Let $r_k(s)$ be the distance from $\mathcal{D}_t$ to the cellular base station which was initially the k-th closest [2] ($\mathcal{C}_k$) after moving for s time slots. Via the cosine rule, we can write

$$r_k(s) = \sqrt{r_k^2 + (vsT)^2 + 2vsTr_k \cos\theta}. \tag{7}$$

Let ρ_k be the probability that $\mathcal{C}_k$ is within a distance of r_j from $\mathcal{D}_t$ after moving for s time slots. Thus, we obtain

$$\begin{aligned} \rho_k &= \Pr[r_k(s) < r_j] \\ &= \Pr\left[r_k < \sqrt{\left(\frac{P}{P_\gamma}\right)^{\frac{2}{\alpha}} + (vsT)^2(\cos^2\theta - 1)} - vsT\cos\theta \right] \\ &= \mathbb{E}_\theta \left[1 - \sum_{i=0}^{k-1} \frac{(\lambda_{cb}\pi U^2)^i}{i!} e^{-\pi \lambda_{cb} U^2} \right], \end{aligned} \tag{8}$$

[2] This base station may not necessarily be the k-th closest after $\mathcal{D}_t$ moves.

This article has been accepted for publication in a future issue of this journal, but has not been fully edited. Content may change prior to final publication. Citation information: DOI 10.1109/TGCN.2020.2994513, IEEE Transactions on Green Communications and Networking

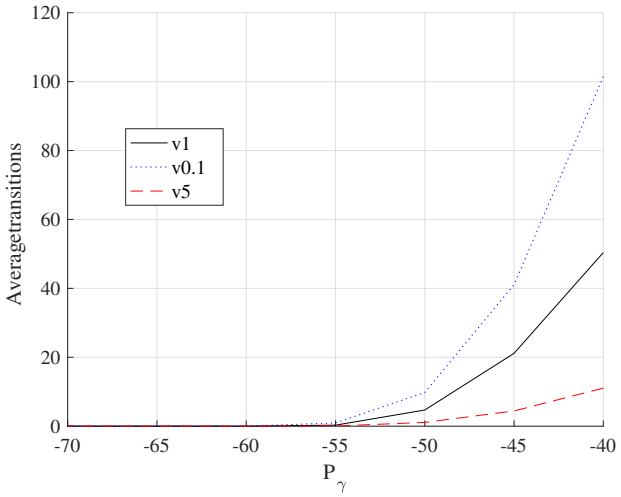

Fig. 3: The average number of transitions (W) vs. P_γ for different v. $\lambda_{cb} = 0.003$.

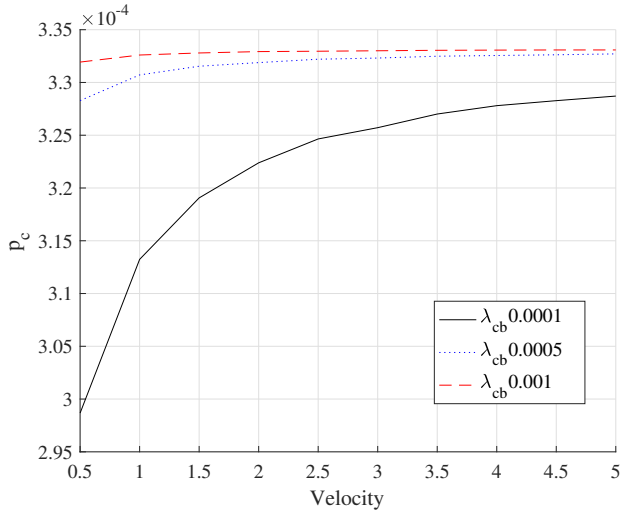

Fig. 4: p_c vs. the velocity (v) for different λ_{cb}. $P_\gamma = -50$ dB.

where $U = \sqrt{\left(\frac{P}{P_\gamma}\right)^{\frac{2}{\alpha}} + (vsT)^2(\cos^2\theta - 1)} - vsT\cos\theta$. Even if a single base station is within r_j, $\mathcal{D}_t$ will be able to harvest energy. Therefore, we can write q_s as

$$q_s = 1 - \prod_{k=1}^{\infty}(1 - \rho_k). \tag{9}$$

V. Numerical Results

This section presents numerical results for p_c and the average number of transitions (W) under different system parameters. Simulation is conducted in MATLAB under $P = 1$, $T = 1$, $\nu = 0.5$, $N = 5$, and $\alpha = 3$.

Fig. 3 plots the average number of transitions required to harvest energy with respect to the energy harvesting threshold P_γ. The average number of transitions increase steadily with P_γ for all the velocities considered, and is extremely low when $P_\gamma < -55$ dB. However, the higher the velocity, the lower the number of transitions required. Given that $\mathcal{D}_t$ is outside the harvesting zone $\mathcal{H}$, there is a higher probability that $\mathcal{D}_t$ is still outside $\mathcal{H}$ after a transition when v is low due to correlations.

The probability of $\mathcal{D}_t$ being at state N at steady state (p_c) is plotted in Fig. 4 with respect to the velocity (v). Increasing the velocity slightly increases p_c, but the rate of increase also diminishes. The value at which the curves flatten out is the value if $\mathcal{D}_t$ sees a new realization of Φ_{cb} after each transition. Moreover, the effect of velocity is higher for lower base station densities; the change in p_c when $\lambda_{cb} = 0.001$ is minute. With a high density of base stations, $\mathcal{D}_t$ has a higher chance of arriving within $\mathcal{H}$ irrespective of the velocity.

VI. Conclusion

This paper investigated the energy harvesting performance of a mobile D2D device powered by ambient RF signals emitted by cellular base stations. A homogeneous Poisson point process was used to model the cellular base stations, and log-distance path loss was considered. Furthermore, the motions of D2D devices followed a modified random waypoint model. The D2D devices were assumed to transition to a new location within discrete time slots until they came within a harvesting zone, and each device needed N time slots within a zone to be fully charged. Using a Markov chain based approach, the steady-state probability of being fully charged was derived. Through numerical results, it is concluded that higher velocities and base station densities reduce temporal correlations, thus reducing the required time slots for transitions and increasing p_c.

References

[1] M. Peng, Y. Li, T. Quek, and C. Wang, "Device-to-device underlaid cellular networks under Rician fading channels," *IEEE Trans. Wireless Commun.*, vol. 13, no. 8, pp. 4247–4259, Aug 2014.

[2] S. Atapattu and J. Evans, "Optimal energy harvesting protocols for wireless relay networks," *IEEE Trans. Wireless Commun.*, vol. 15, no. 8, pp. 5789–5803, Aug 2016.

[3] R. Atat, L. Liu, N. Mastronarde, and Y. Yi, "Energy harvesting-based D2D-assisted machine-type communications," *IEEE Trans. Commun.*, vol. PP, no. 99, pp. 1–1, 2016.

[4] S. Lee, R. Zhang, and K. Huang, "Opportunistic wireless energy harvesting in cognitive radio networks," *IEEE Trans. Wireless Commun.*, vol. 12, no. 9, pp. 4788–4799, September 2013.

[5] S. Kusaladharma and C. Tellambura, "Energy harvesting random underlay cognitive networks with power control," in *Proc. IEEE ICC*, May 2017, pp. 1–6.

[6] S. Kusaladharma and C. Tellambura, "Performance characterization of spatially random energy harvesting underlay D2D networks with primary user power control," in *Proc. IEEE ICC*, May 2017, pp. 1–6.

[7] A. Sakr and E. Hossain, "Cognitive and energy harvesting-based D2D communication in cellular networks: Stochastic geometry modeling and analysis," *IEEE Trans. Commun.*, vol. 63, no. 5, pp. 1867–1880, May 2015.

[8] H. H. Yang, J. Lee, and T. Q. S. Quek, "Heterogeneous cellular network with energy harvesting-based D2D communication," *IEEE Trans. Wireless Commun.*, vol. 15, no. 2, pp. 1406–1419, Feb 2016.

[9] K. Huang, M. Kountouris, and V. O. K. Li, "Renewable powered cellular networks: Energy field modeling and network coverage," *IEEE Transactions on Wireless Communications*, vol. 14, no. 8, pp. 4234–4247, Aug 2015.

[10] D. B. Licea, S. A. R. Zaidi, D. McLernon, and M. Ghogho, "Improving radio energy harvesting in robots using mobility diversity," *IEEE Trans. Signal Process.*, vol. 64, no. 8, pp. 2065–2077, April 2016.

[11] J. F. Kingman, *Poisson Processes*. Oxford University Press, 1993.

[12] S. Kusaladharma, P. Herath, and C. Tellambura, "Underlay interference analysis of power control and receiver association schemes," *IEEE Trans. Veh. Technol.*, vol. 65, no. 11, pp. 8978–8991, Nov 2016.

[13] S. Kusaladharma and C. Tellambura, "Study of mobility in cache-enabled wireless heterogeneous networks," in *Proc. IEEE WCNC*, Mar 2017, pp. 1–6.

[14] X. Lin, R. K. Ganti, P. J. Fleming, and J. G. Andrews, "Towards understanding the fundamentals of mobility in cellular networks," *IEEE Trans. Wireless Commun.*, vol. 12, no. 4, pp. 1686–1698, April 2013.

[15] D. Moltchanov, "Distance distributions in random networks," *Ad Hoc Networks*, vol. 10, no. 6, pp. 1146–1166, 2012. [Online]. Available: http://www.sciencedirect.com/science/article/pii/S1570870512000224